SPECTROSCOPIC IDENTIFICATION OF IMPLANTED SOLAR WIND HELIUM IN VESICLES IN LUNAR ILMENITE. K. D. Burgess[1] and R. M. Stroud[1], [1]Naval Research Laboratory, 4555 Overlook Ave. SW, Washington, DC 20375. (kate.burgess@nrl.navy.mil)

Introduction: The solar wind is a major driver of space weathering on airless bodies and has been implicated in amorphization, compositional changes, nanophase metallic iron ($npFe^0$) inclusion formation, and the formation of vesicle-rich rims in lunar and asteroidal material and interplanetary dust particles (IDPs) [1-3]. The trapping of solar wind-implanted hydrogen in planetary materials has implications for the formation and delivery of water on the Moon and to terrestrial planets [2], while trapped helium has been suggested as a valuable resource in future space exploration [4] and contributes to anomalous He isotope ratios in some deep sea sediments [5].

Of the most common phases on the lunar surface (plagioclase, pyroxene, olivine, silicate glass, ilmenite), ilmenite is both the most resistant to sputtering and amorphization by ion irradiation [6] and the most retentive of implanted He [7]. Thus, lunar ilmenite can serve as a record of solar wind He and other noble gas isotope ratios throughout much of the history of the solar system [8,9] and provide a basis for locating helium reserves on the Moon [10]. Understanding how helium and other solar wind ions are trapped in minerals and glasses is key to interpreting noble gas abundance ratios and trends within and between various planetary materials [11].

Vesicles present in space weathered rims of some lunar soil grains seen in transmission electron microscopy (TEM) and surface blisters observed via scanning electron microscopy (SEM) are inferred to be due to the build-up of solar wind H and He. Water (i.e., hydrogen) has been tentatively identified in vesicles in space weathered rims of an IDP [2]. However, helium has not been identified in naturally implanted materials. In the current study, we use spatially resolved electron energy loss spectroscopy (EELS) in a scanning transmission electron microscope (STEM) to demonstrate the presence of helium in vesicles in the space weathered rim of a lunar ilmenite grain and link the bubble characteristics to other previously observed space weathering features.

Methods: Samples were prepared using focused ion beam (FIB) microscopy. An ilmenite grain from lunar soil 71501 was coated with a thick carbon film (1-2 µm) before ion milling to prevent damage to the grain surface by the ion beam. The thinned sections were moved directly from the FIB to the pre-bake vacuum chamber where they were heated to 140°C for six hours to drive off adsorbed water before insertion in the UHV system.

Equipment. Electron energy loss spectroscopy (EELS) and energy dispersive x-ray spectroscopy (EDS) data were collected with PRISM, the NION UltraSTEM200-X at the U.S. Naval Research Laboratory, equipped with a Gatan Enfinium ER EEL spectrometer with and a Bruker SSD-EDS detector. The STEM was operated with at 200 kV, with a 0.1 to 0.2 nm probe. Spectra were collected as spectrum images (SI), with a spectrum collected for each pixel, allowing for mapping of variations in thickness and composition.

Results: The FIB sections expose multiple original grain surfaces in different orientations, and significant differences are seen in defect areal density and vesicle number in different regions. Solar flare tracks are not observed, but 71501 has a bulk cosmic ray exposure age ~100 Myr [7]. However, individual soil grains can be highly variable, and helium saturation and bubble formation could occur in <500 yr [9]. The general morphology closely resembles that observed previously in lunar and experimentally irradiated ilmenite [12,13], with the space weathered rim consisting of a disordered outer layer 35-40 nm thick and rich in $npFe^0$ inclusions on most of the grain, covering an inner, defect-rich layer extending 70-100 nm into the grain (Fig. 1). The defects in the inner layer are aligned on the (001) plane of the ilmenite, regardless of the orientation of the exposed face. The outer layer of the ilmenite also contains a number of vesicles (Fig. 1). The sample was categorized into four regions based on surface orientation and extimates of exposure (Fig. 2). At least 14 different bubbles, or vesicles still containing He, were measured.

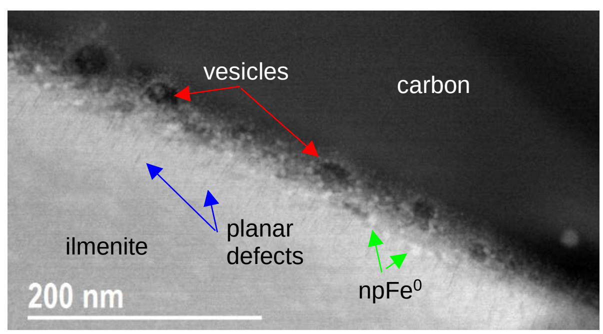

Figure 1. HAADF image of the space weathered rim of an ilmenite grain, showing the presence of large vesicles, some of which still contain helium implanted by the solar wind, in a disordered, $npFe^0$-rich rim, extending into a Si-rich vapor deposited rim. Planar defects here seen perpendicular to the exposed surface extend to a depth of ~90 nm and are aligned on the (001) plane of ilmenite regardless of orientation of the exposed surface.

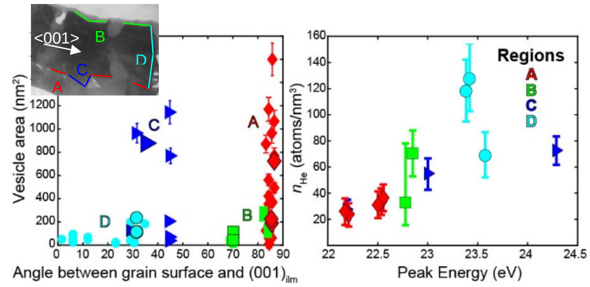

Figure 2. (a) The ilmenite surface was categorized by the angle between the surface and the (001) plane and the size of the observed vesicles. A and C appear to have had the most exposure to the solar wind and have high defect and vesicle areal density. **(inset)** Low-magnification image of FIB section. **(b)** The energy of the helium peak can shift >2 eV with increasing bubble pressure. The helium density is highest in regions where the (001) plane intersects the surface at angles <50°.

The concentration of helium trapped in the bubbles ranges from 20-130 He/nm^3 based on the method of Walsh et al. [14], and peak energies range from 22.0 eV to 24.3 eV (Fig. 2). Although significant uncertainty is introduced to the density calculation by the estimation of the bubble thickness, calculated from EELS low-loss spectra inside relative to outside the bubble, the energy shift of the peak center is consistent with a large range in helium density. Two bubbles of different size and He density are highlighted in Fig. 3.

Conclusion: Trapped gases have economic and exploration implications, as well as providing information for understanding trapping and release mechanisms of implanted ions in planetary material, material processing in different regions of the solar system and how the effects of space weathering could change depending on location and distance from the Sun. Data from nanobubbles in individual grain rims, revealed by FIB/STEM, can provide key information on material response to irradiation and subsequent processing, such as heating.

Acknowledgements: This work was supported by the RIS[4]E node of NASA's Solar System Exploration Research Virtual Institute.

References: [1] Keller, L.P., and D.S. McKay (1997) *GCA*, *61*, 2331. [2] Bradley, J.P., et al. (2014) *PNAS*, *111*, 1732. [3] Noguchi, T., et al. (2014) *M&PS*, *49*, 188. [4] Wittenberg, L., et al. (1986) *Fusion Sci Technol*, *10*, 167. [5] Merrihue, C. (1964) *Ann NY Acad Sci*, *119*, 351. [6] Futagami, T., et al. (1993) *GCA*, *57*, 3177. [7] Signer, P., et al. (1977) *LPSC*, *8*, 3657-3683. [8] Heber, V.S., et al. (2003) *Astrophys J*, *597*, 602. [9] Nichols, R., et al. (1994) *GCA*, *58*, 1031. [10] Johnson, J.R., et al. (1999) *GRL*, *26*, 385. [11] Wieler, R., et al. (2006) In: *Meteorites and the Early Solar System II*. 499-521. [12] Christoffersen, R., et al. (2010) *LPSC*, *41*, 1532. [13] Christoffersen, R., et al. (1996) *M&PS*, *31*, 835. [14] Walsh, C.A., et al. (2000) *Philos Mag A*, *80*, 1507.

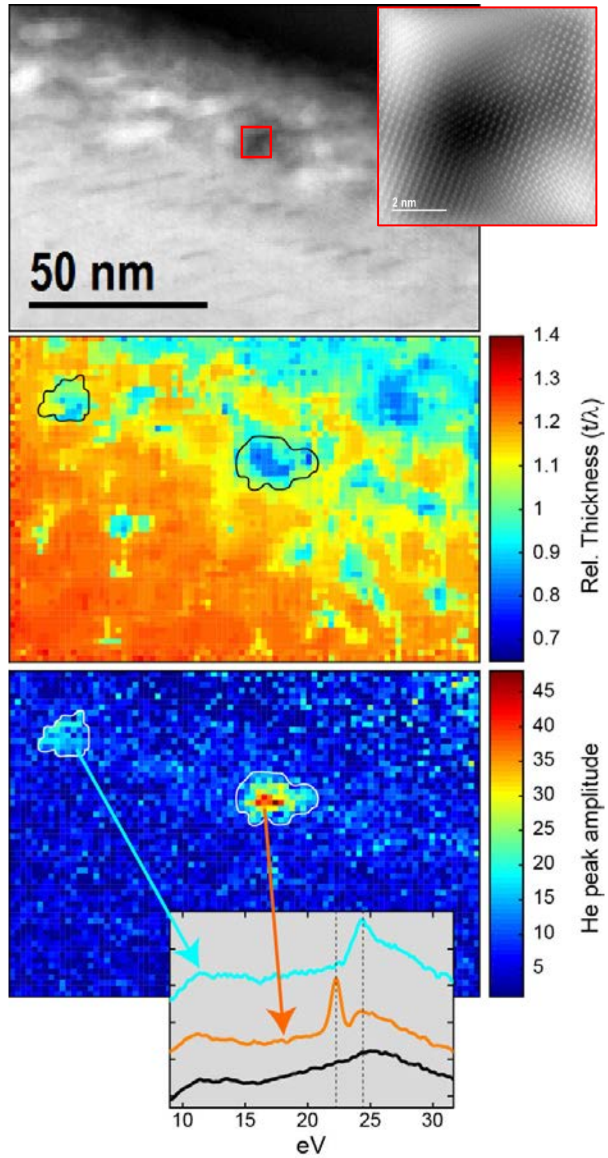

Figure 3. The top HAADF image shows a section of the ilmenite surface in region C with two helium-filled bubbles in the disordered outer layer. Planar defects aligned with ilmenite (001) are present in the inner layer. The inset shows an inverse FFT pattern for the larger bubble, showing the surrounding ilmenite is crystalline. The maps are calculated using the EELS signal, showing the relative change in thickness of the bubbles and the amplitude of a Gaussian peak fit to the extracted helium signal. Spectra summed over each of the two bubbles are shown with an ilmenite plasmon spectrum (black) for comparison (offset for clarity). The shift in energy between the two bubbles indicates different interior pressure of helium.